

Characterization of Fresh and Decomposed Dissolved Organic Matter Using Excitation–Emission Matrix Fluorescence Spectroscopy and Multiway Analysis

JAMES F. HUNT AND TSUTOMU OHNO*

Department of Plant, Soil, and Environmental Sciences, University of Maine,
 5722 Deering Hall, Orono, Maine 04469-5722

Fresh and decomposed dissolved organic matter (DOM) derived from 13 plant biomass and animal manure sources was characterized using multidimensional fluorescence spectroscopy with parallel factor analysis (PARAFAC), high-performance size-exclusion chromatography, and UV–vis spectroscopy. The PARAFAC analysis modeled seven fluorescence components: tryptophan-like, tyrosine-like, and five humic substance-like components. For most of the plant-derived DOM solutions, decomposition significantly affected the concentration of three humic substance-like-associated components, increasing two and decreasing one. The effect of decomposition upon DOM derived from animal manures was dependent on the manure source. For a majority of the DOM extracts, the ratio of fluorescence intensity to absorptivity at 254 nm increased following decomposition, indicating that fluorescing DOM compounds were generally more resistant to biodegradation than nonfluorescing UV-absorbing compounds. Molar absorptivity, humification index (HIX), and apparent molecular weight (MW_{AP}) increased by 38.0, 38.8, and 370%, respectively, following decomposition. Spearman correlation analysis showed a strong positive relationship between the humic substance-like components and the DOM MW_{AP} , absorptivity, and HIX. The results of this study support the use of multidimensional fluorescence spectroscopy with PARAFAC as a method to monitor the decomposition of carbon-rich soil amendments such as crop residues, green manures, and animal manures.

KEYWORDS: Dissolved organic matter; plant biomass; animal manures; multidimensional fluorescence spectroscopy; multiway analysis; PARAFAC

INTRODUCTION

The incorporation of crop residues and animal manures into soils is an important agricultural management technique for maintaining soil quality and nutrient availability through the replenishment of C to soil ecosystems. Cropping system studies have shown that levels of both total soil organic matter and dissolved organic matter (DOM) are influenced by the type of organic amendment used (1, 2). The added DOM fraction from fresh or early stage decomposing soil amendment materials may play an important role in many chemical processes due to its mobility and reactivity with both soil solution components and soil surfaces. The chemical properties of DOM have been characterized using a variety of methods. The determination of DOM apparent molecular weight (MW_{AP}) by high-performance size-exclusion chromatography with UV detection has become a widely used technique (3, 4). In this method, DOM retention times are converted to MW_{AP} using a calibration curve comprised of known molecular weight standards, and the

magnitude of the UV absorbance at each time unit is taken to be proportional to the mass frequency of the associated chromophore (5). The aromaticity of DOM can be inferred from its molar absorptivity at UV wavelengths of 280 nm or less, as well by the ratio of its UV absorbance at 250 nm to that at 365 nm (E2/E3 ratio) (6).

Fluorescence spectroscopy is a sensitive, rapid, and nondestructive technique that has been used to characterize the nature of DOM. In emission mode, it can provide a measure of the extent of humification by quantifying the red shifting of emission spectra toward longer wavelengths at a fixed excitation wavelength of 254 nm (7, 8). Excitation–emission matrix (EEM) fluorescence spectroscopy measures the emission spectra over a wide range of excitation wavelengths, resulting in a fluorescence intensity landscape defined by the excitation and emission wavelength ranges. EEM fluorescence spectroscopy has been used to characterize fluorophores in diverse samples, such as those obtained from surface waters (9), wastewaters (10), sludge (11), leaf litter (12), crop residues (13), and soil (14–16). Recent advances utilizing parallel factor analysis (PARAFAC), a multiway analysis technique, have greatly improved the utility

* To whom correspondence should be addressed. Tel: +1 207-581-2975. Fax: +1 207-581-2999. E-mail: ohno@maine.edu.

of the EEM method by modeling data into spectral and concentration components. These chemometric models allow for a robust description of sample fluorophores, making possible quantitative comparisons of the samples in the data set.

Studies with soil DOM have shown that resistance to biodegradation is generally associated with DOM of high hydrophobicity and aromatic content, as well as low DOM carbohydrate content (17, 18). Increases in aromaticity, molecular complexity, and MW_{AP} with biodegradation were reported from a variety of DOM sources (17). In contrast, a study by Marschner and Bredow (19) reported that specific UV absorbance did not correlate well with DOM biodegradability, leading the authors to propose that nonaromatic compounds may also vary significantly in biodegradability depending upon their degree of polymerization or oxidation. Because fluorescing compounds comprise only a small percentage of the total pool of UV-active DOM compounds, they represent another means of monitoring the changes produced by biodegradation. Previous studies with effluent, freshwater, and marine DOM samples have shown postdecomposition changes in carbon-normalized fluorophore concentrations in peaks associated with both humic materials (20) and bacterially generated, tryptophan-like materials (21, 22). Recent research involving DOM derived from green/animal manure-amended and nonamended agricultural soils showed little variation in relative fluorophore concentrations between the two groups of soils, while DOM derived from fresh plant and animal manure varied widely in fluorophore characteristics (12). This suggests that while certain organic amendments do raise the organic content of soils, they do not affect the fluorescing components of DOM.

The primary objective of this study is to evaluate the use of EEM fluorescence spectroscopy and PARAFAC to determine changes in the chemical nature of DOM derived from plant biomass and animal manures following microbial decomposition. In addition, the relationship between the PARAFAC-derived DOM components to other readily measurable parameters such as molecular weight, humification index (HIX), and UV absorptivity was investigated. Knowledge of the chemical changes occurring to DOM during the decomposition of these soil amendments could significantly assist in the sound environmental management of agricultural resources.

MATERIALS AND METHODS

DOM Sources. Field-weathered above-ground portions of oat (*Avena sativa* L.), millet (*Panicum miliaceum* L.), soybean [*Glycine max* (L.) Merr.], corn (*Zea mays* L.), and wheat (*Triticum aestivum* L.) were obtained from cropping system studies in Maine, Kansas, and Iowa. Above-ground portions of field-grown hairy vetch (*Vicia villosa* L.), crimson clover (*Trifolium incarnatum* L.), alfalfa (*Medicago sativa* L.), canola (*Brassica napus* L.), and lupin (*Lupinus albus* L.) were obtained from a cropping system study in Maine. All plant samples were air-dried and ground to pass a 1 mm sieve. The dairy and poultry manures were obtained from farms in Maine, while the swine manure sample used was described previously by Griffin and Honeycutt (23). All manure samples were air-dried and sieved through a 2 mm metal mesh. The fresh DOM from these materials was obtained by extracting the materials at a 40:1 (v:w) water to residue ratio using cold deionized distilled water (DI-H₂O) and refrigerating (4 °C) the mixtures for 18 h with periodic hand shaking. Suspensions were then centrifuged (900g) for 30 min prior to vacuum filtering through 0.4 μm polycarbonate filters.

Decomposition. Decomposition of the plant biomass and manure was conducted using a procedure modified from Merritt and Erich (13). Briefly, 2.00 g of plant or manure sample and 10 mL of DI-H₂O were added to 36 g of acid-washed silica sand in 125 mL polyethylene screw-top bottles. Thirty microliters of a fresh field soil extract (1 g of soil

+ 10 mL of DI-H₂O) was added to each bottle to provide a microbial population representative of fresh field soils. To assess any possible contribution of DOM from the soil inoculum, control vials containing silica, DI-H₂O, and soil inoculum were prepared. The C/N ratios were determined for the plant and manure samples using a LECO CN-2000 carbon-nitrogen analyzer, and ammonium nitrate was added as necessary to attain a C/N ratio of approximately 20 for each sample prior to incubation. This was done to ensure that decomposition was not limited by N availability. The bottles were loosely capped and placed in the dark at room temperature. Bottles were weighed, and DI-H₂O was added, as necessary, on alternate days to maintain the initial moisture level. The decomposed DOM was extracted on day 10 in the same manner as for the fresh samples. Two replicates of each material and control were analyzed.

Chemical Characterization. The concentrations of total-soluble organic carbon (C_{TS}) in each DOM solution were determined using a Shimadzu 5000 Carbon Analyzer. Each extract was then diluted to 30 mg C_{TS} L⁻¹. Ultraviolet-visible spectra were recorded using an Agilent 8453 diode array spectrophotometer with a 1 cm quartz cuvette. The UV absorbance values at 254, 280, and 365 nm were used to calculate the molar absorptivities at 280 nm (absorbance at 280 nm divided by the C molar concentration) and the E2/E3 ratios (absorbance at 254 nm divided by absorbance at 365 nm) of each sample (6). Molar absorptivity at 280 nm has been found to correlate well with DOM aromaticity, and the E2/E3 ratio has been shown to be inversely related to DOM molecular weight (5).

High-performance size-exclusion chromatography was used to estimate the MW_{AP} of the DOM. The system consisted of a Hewlett-Packard (Agilent, San Jose, CA) 1100 high-performance liquid chromatography unit equipped with a G1311A quaternary pump, a G1314 autosampler, and a G1315A photodiode array UV detector. A Waters Protein Pak 125 stainless steel SEC column with a Waters guard column was used. The mobile phase consisted of a 0.1 M NaCl aqueous solution buffered to pH 6.8 with 5 mM phosphate buffer. Samples were matched to the mobile phase matrix by the addition of 0.1 mL of 1 M NaCl solution (phosphate buffered to pH 6.8) to 0.9 mL of sample. Calibration of molecular weight to retention time was accomplished using polystyrene sulfonate sodium standards (2.0 mg mL⁻¹) of nominal masses of 4.6, 8.0, and 18.0 kDa and polydispersity values of less than 1.2 (Polymer Laboratories, Silver Spring, MD). Benzoic acid and salicylic acid were used as the low molecular mass standards in the calibration. The injection volume for all samples was 100 μL, and the flow rate was 1.0 mL min⁻¹ with detection at 230 and 254 nm (5). All standards and samples were analyzed in duplicate.

EEM Fluorescence and PARAFAC. Fluorescence measurements were obtained using a Hitachi F-4500 spectrofluorometer (Hitachi, San Jose, CA) with the excitation range set from 240 to 400 nm and the emission range set from 300 to 500 nm in 3 nm increments. Instrumental parameters were as follows: excitation and emission slits, 5 nm; response time, 8 s; and scan speed, 240 nm/min. The HIX value was calculated as: $HIX = (\sum I_{435/480}) / (\sum I_{300/345})$, where I is the fluorescence intensity at each wavelength using an excitation wavelength of 254 nm (8).

Preprocessing steps were used to minimize the influence of scatter lines and other attributes of the EEM landscape before PARAFAC modeling. An EEM that was collected from a control DI-H₂O solution was subtracted from each sample EEM to remove the lower intensity Raman scatter effects (24). The blank subtraction will not adequately remove the higher intensity Rayleigh scatter lines. Thus, the Rayleigh scatter lines and the region immediately adjacent to the region where the emission and excitation wavelengths are equal were removed by setting the fluorescence intensity values of these data points as missing. In addition, EEM data have a triangular-shaped region where the emission wavelength is less than the excitation wavelength (upper left-hand corner), which is physically impossible, and these data pairs were set to zero.

The PARAFAC modeling approach has been described in detail elsewhere (25). The PARAFAC modeling was conducted with MATLAB, Release 14 (Mathworks, Natick, MA) using PLS_Toolbox version 4.0 (Eigenvector Research, Manson, WA). A non-negativity constraint was applied to the parameters to allow only chemically relevant results

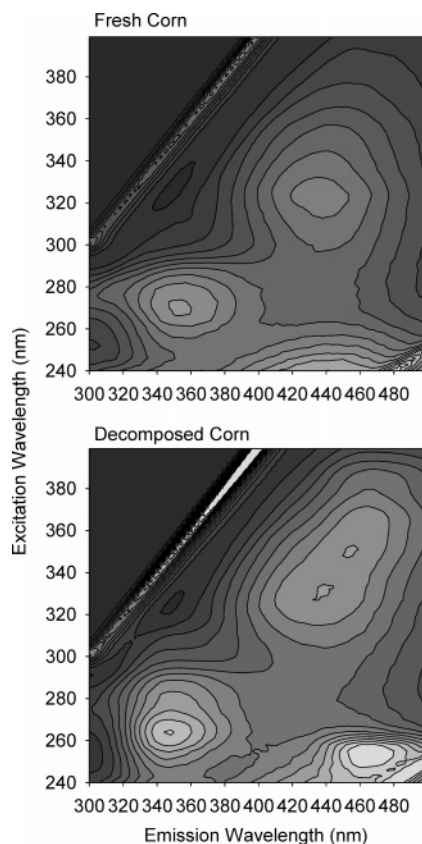


Figure 1. Full scan EEM fluorescence spectrum for fresh and decomposed corn residue-derived DOM.

because negative concentrations and fluorescence intensities are chemically impossible assuming that quenching and inner filter effects are negligible. PARAFAC models with 5–10 components were computed. The correct number of components in the data set was determined by the core consistency diagnostic score, which should be close to 100% for appropriate models. The core consistency provides an estimate of how well the model captures trilinear information, and if the consistency turns low, i.e., toward zero, it is a strong indication that the model is invalid (25).

Statistical Analysis. Spearman rank-order correlations were used to examine the relationships between the component scores determined by PARAFAC and the independently measured DOM chemical characteristics of molar absorptivity, MW_{AP} , DOM content, E2/E3 ratio, and HIX. Student *t* tests were used for measuring the statistical significance of the differences between the fresh and the decomposed DOM chemical characteristics. All statistical analyses were conducted using the software package SAS 9.1 for Windows.

RESULTS AND DISCUSSION

Multidimensional Fluorescence Spectroscopy. The full-scan fluorescence landscape with excitation ranging from 240 to 400 nm and emission ranging from 300 to 500 nm was determined for each fresh and decomposed DOM sample. **Figure 1** shows the fresh and decomposed corn as representative landscapes for plant biomass-derived DOM. The “peak picking” approach suggests the potential presence of four fluorophores in the fresh corn DOM centered at excitation and emission wavelength pairs of <240/440 nm, 250/300 nm, 270/355 nm, and 320/440 nm. Visual changes in the landscape for the decomposed corn DOM can be seen, with evidence of a new fluorophore at 250/465 nm and substantial broadening of the 320/440 nm fluorophore. The EEM spectra of fresh and decomposed poultry manure-derived DOM are shown in **Figure 2**. Three fluorophores can be visually identified for the fresh (<240/440 nm, 270/350 nm,

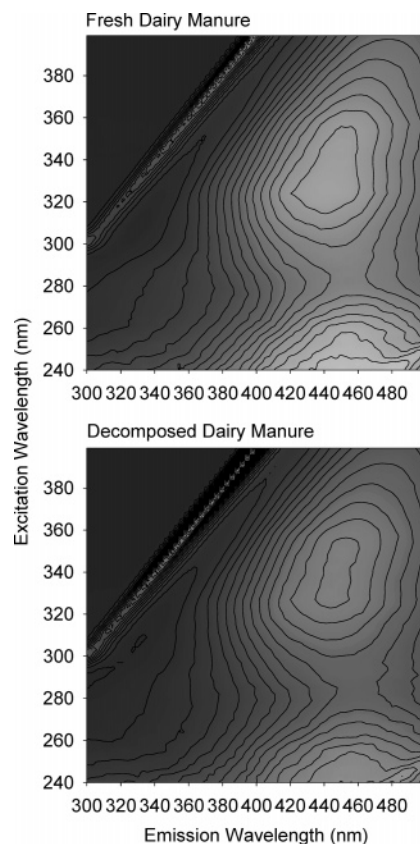


Figure 2. Full scan EEM fluorescence spectrum for fresh and decomposed poultry manure-derived DOM.

and 330/430 nm) and the decomposed poultry manure DOM (355/440 nm, 260/345 nm, and 250/465 nm).

PARAFAC Modeling. The three-way PARAFAC model is ideal for analyzing a suite of EEM spectra because of the inherent two-way nature of the EEM (number of excitation wavelengths \times number of emission wavelengths), with samples as the third way. A prior study using a similar set of fresh DOM materials was modeled successfully with five PARAFAC components (12). For this combined set of fresh and decomposed DOM, PARAFAC models with 5–10 components were computed. The most appropriate number of components to use was assessed using the core-consistency diagnostic score, which should be close to 100% for appropriate models. The core-consistency diagnostic scores for the 5–10-component models were 66.7, 34.7, 80.5, –60.9, –2150, and –4760, respectively. The seven-component model, which explained >99% of the EEM data variability in this study, was therefore selected as the appropriate PARAFAC model to describe the data set. The additional two components needed to model this fresh and decomposed DOM data set, as compared to the similar fresh-only DOM set (12), likely reflects, in some part, byproducts of the microbial processes decomposing the amendment sources (26).

The excitation and emission spectral loadings for the seven components are shown in **Figure 3**. Although individual instrumental biases and variations in chemometric processing procedures employed by different investigators result in problematic interlaboratory comparisons of components (27), many studies have confirmed that DOM derived from various environments have qualitatively similar fluorescence components, due to the presence of humiclike substances and protein-containing aromatic amino acids (28, 29). Components 2–4 and 6 have two excitation spectral peaks and a single emission peak,

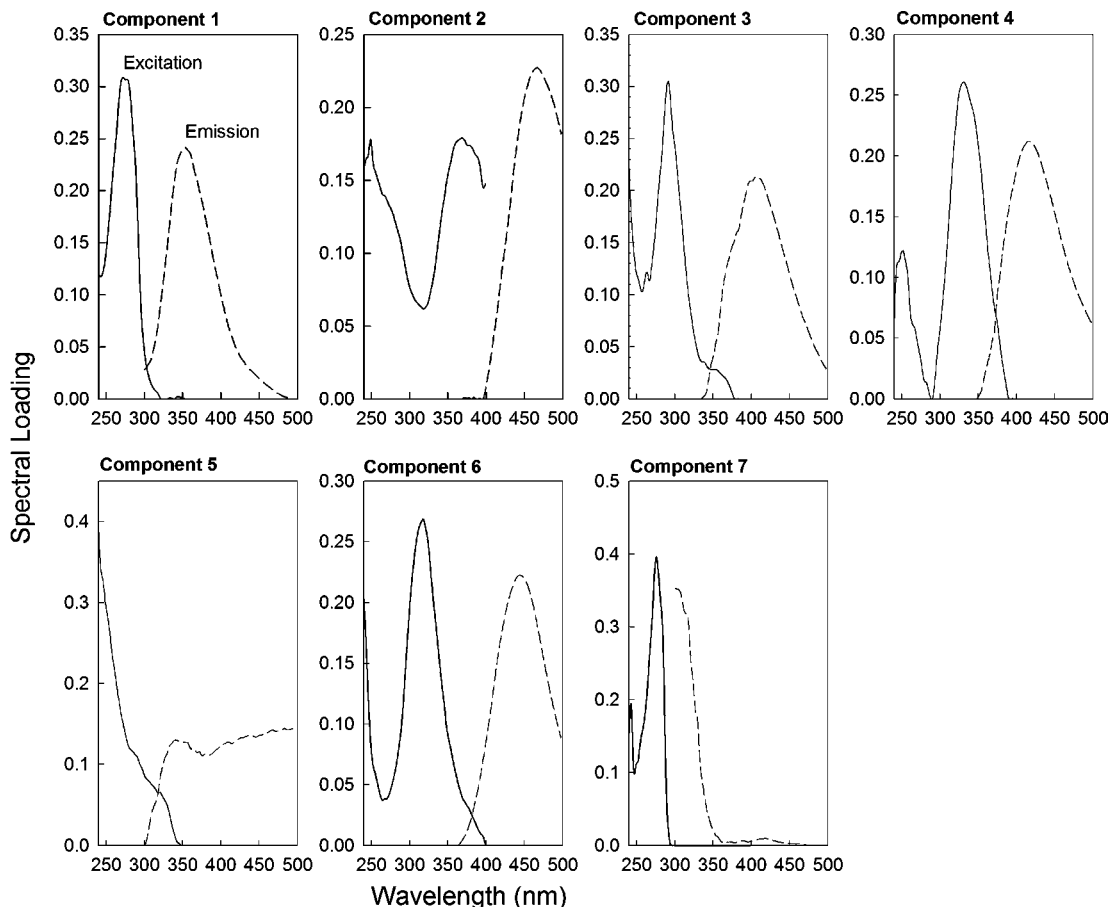


Figure 3. Excitation and emission spectral loadings of the non-negativity constrained seven-component PARAFAC model of the fresh and decomposed DOM data set.

which is a characteristic that has been widely reported with humic substances (12, 15). In addition, these four components have spectral peaks in wavelength ranges associated with humic materials in a classification reported by Leenheer and Croué (30). Components 1 and 7 have been found in many previous studies of natural organic matter (12, 31) and are generally accepted to be associated with proteins containing free tryptophan and tyrosine, respectively (30). Component 5 (240/489 nm) has a single peak excitation wavelength similar to that of the primary peaks of both components 2 and 3, with an emission spectra that is red-shifted into a range that approximately corresponds to an often observed, but poorly defined, component, sometimes referred to as the “A” peak (32).

The scores from the first loading of the PARAFAC model are an estimate of the component concentrations for each DOM sample. These scores are based upon the signal intensities of the components present in each sample and do not represent actual chemical concentrations. Expressing actual chemical concentrations would require knowledge of the quantum efficiencies of all fluorophores in the complex mixture of compounds present in each DOM. Thus, a strongly emitting component present in low chemical concentration could contribute more to the modeled overall component concentration than a weak-emitting fluorophore of much higher chemical concentration. These signal-based concentrations, however, can be used to access how decomposition alters the chemical nature of the DOM.

The effect of decomposition upon the concentration of components found in extracts normalized to 30 mg C_{TS} L⁻¹ is shown for plant biomass and animal manure DOM in Table 1. The data illustrate both the wide variation in component

concentrations among the DOM samples and the dissimilar effects of decomposition upon these components. Component 2 had significantly higher intensities in the decomposed DOM for 8 of the 10 plant biomass-derived DOM. Component 4 also had significantly higher concentrations in the decomposed DOM for 7 of the 10 plant biomass DOM. Component 7, the tyrosine-containing fluorophore, had a significantly higher concentration in five plant biomass-derived DOM and a significantly lower concentration in two of the plant DOM. Component 6 significantly decreased in concentration in 8 of the 10 plant biomass-derived DOM. The direction of changes in component concentrations upon decomposition was generally consistent, allowing for the meaningful calculation of percentage changes in the concentration of plant biomass DOM (Figure 4). Decomposition altered the concentration of components 1, 3, and 5 less than ~5%. The increase in two of the “humic-like” components 2 and 4 following microbial decomposition suggests that the remaining DOM is more condensed, as the simpler forms of organic compounds are presumably utilized as energy sources.

The decomposition effects on animal manure DOM were not consistent among the sources (Table 1). Components 2–4 significantly increased in concentration following decomposition for poultry and swine manure-derived DOM but significantly decreased for dairy manure-derived DOM. Component 6 decreased for dairy and poultry manure but increased for swine manure. The “tyrosine-like” component 7 decreased for dairy and swine manure but was unchanged for poultry manure. Concentrations of components 1 and 5 were not significantly changed by decomposition. The lack of consistent trends for the animal manure-derived DOM, as compared to the plant-derived DOM, likely reflects variations in the chemical proper-

Table 1. Concentrations (Expressed in Arbitrary Signal Intensity Units) of PARAFAC Components in 30 mg C_{TS} L⁻¹ Samples of Fresh and Decomposed DOM from Plant Biomass and Animal Manures^a

DOM source		component						
		1	2	3	4	5	6	7
		Plant Biomass						
alfalfa	fresh	1140	1412	3501	34.2	644	1771	176
	decomposed	1540	1857***	1570***	1676***	804	1205*	773**
canola	fresh	2385	443	778	156	788	1644	210
	decomposed	1810	1441***	1456***	1442***	1282*	439***	182
corn	fresh	2093	1543	875	1431	1291	1199	505
	decomposed	2742	3330***	460*	2142**	1393	733*	196*
crimson clover	fresh	5535	1683	1039	338	696	1587	289
	decomposed	6043	1864	1032	877*	607	940*	563***
hairy vetch	fresh	4276	607	2226	41.4	693	2651	412
	decomposed	5372	1956***	4370**	1468***	395	1462**	848**
lupin	fresh	3043	809	540	958	1032	404	440
	decomposed	3000	1910**	1073**	1968**	926	268***	365
millet	fresh	681	487	284	265	1268	697	381
	decomposed	332*	1044***	392*	481**	1412	802	126**
oat	fresh	2291	477	398	240	1311	1104	221
	decomposed	2011	469	347	427	1391	672	419*
soybean	fresh	1021	667	806	98.2	915	1183	151
	decomposed	947	1021**	363**	394	1149	437**	252*
wheat	fresh	908	944	918	404	1239	2829	396
	decomposed	457**	1194*	724	1000	1043	1049**	371
		Animal Manure						
dairy manure	fresh	120	3442	1187	1974	1152	965	33.0
	decomposed	33.7	2831**	749**	1526**	495	669*	0**
poultry manure	fresh	2296	2539	491	3049	1009	595	400
	decomposed	2453	5170***	2149***	3600*	1560	2.00**	471
swine manure	fresh	4048	1117	2000	1576	2107	489	3873
	decomposed	3308	2380***	3448**	3057**	3153	999*	1956**

^a *, **, and *** designate significant differences at $p = 0.05$, 0.01 , and 0.001 between fresh and decomposed component concentrations for each extract.

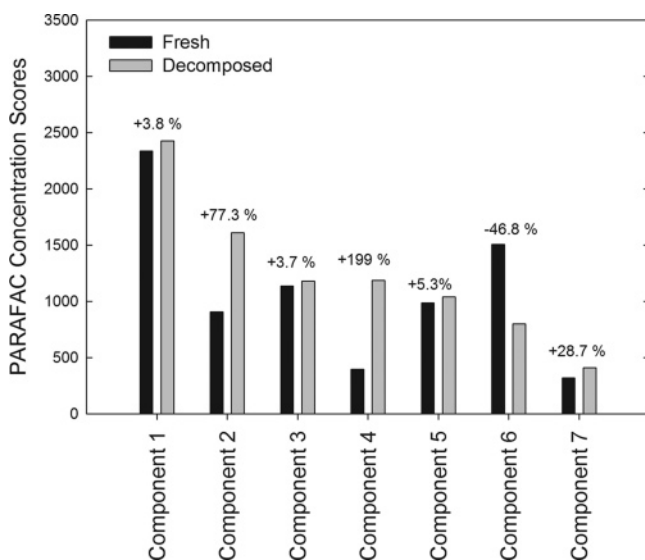


Figure 4. Concentration scores of the seven-component PARAFAC model for the fresh and decomposed plant biomass-derived DOM. Numbers above bars indicate % change in score postdecomposition.

ties of feed materials for the different animals, as well as differing digestive processes of the animals.

Chemical Characteristics of DOM. Carbon-rich soil amendments serve as energy sources for microbes, resulting in the C being respired and released as CO₂, incorporated into microbial biomass, or converted into microbial byproducts. The DOM concentrations of the extracts before and after decomposition, as measured by C_{TS}, are shown in **Table 2**, along with a summary of decomposition-induced changes in other DOM chemical parameters. All plant biomass-derived DOM extracts, with the exception of the oat sample, had lower DOM

concentrations after decomposition, with an average decrease of $30.2 \pm 10.4\%$. Decreases in C_{TS} content during the initial phase of decomposition are due to preferential utilization of the labile sugar, amino acid, and protein fractions of DOM (18). The lower amounts of C_{TS} in the fresh manure extracts relative to that of the plant extracts may be due to animal metabolic utilization of the more soluble C fractions present in the feed (33). Decomposition effects on the three animal manure samples were not consistent, with dairy manure and poultry manure DOM concentrations increasing following decomposition and swine manure decreasing in DOM concentration following decomposition (**Table 2**).

The differential use of DOM components by microbial agents is expected to alter the chemical nature of DOM following decomposition. This change has been documented by others using specific UV absorbance and molecular weight analysis to characterize the DOM following biodegradation (17). The low HIX, molar absorptivity, and MW_{AP} values generally observed for plant-derived DOM were likely due to a high content of polysaccharides and other weakly chromophoric biomolecules present (2). The PARAFAC results indicated a general increase in the “humic-like” components following decomposition for the plant-derived DOM, and the data in **Table 2** support that finding with these parameters, also indicating a more humified, postdecomposition DOM chemical structure. For the **Table 2** data set as a whole, molar absorptivity, HIX, and MW_{AP} increased by means of 38.0, 38.8, and 370%, respectively. Comparable trends have also been observed in the biodegradation of wastewater (20), spent mushroom substrate (6), and soil-derived DOM (17, 19). These trends indicate either selective degradation of DOM of lower aromaticity and molecular weight or decomposition processes that synthesize

Table 2. Selected Chemical Parameters of Fresh and Decomposed Field-Weathered and Legume Plant Residues and Animal Manures^a

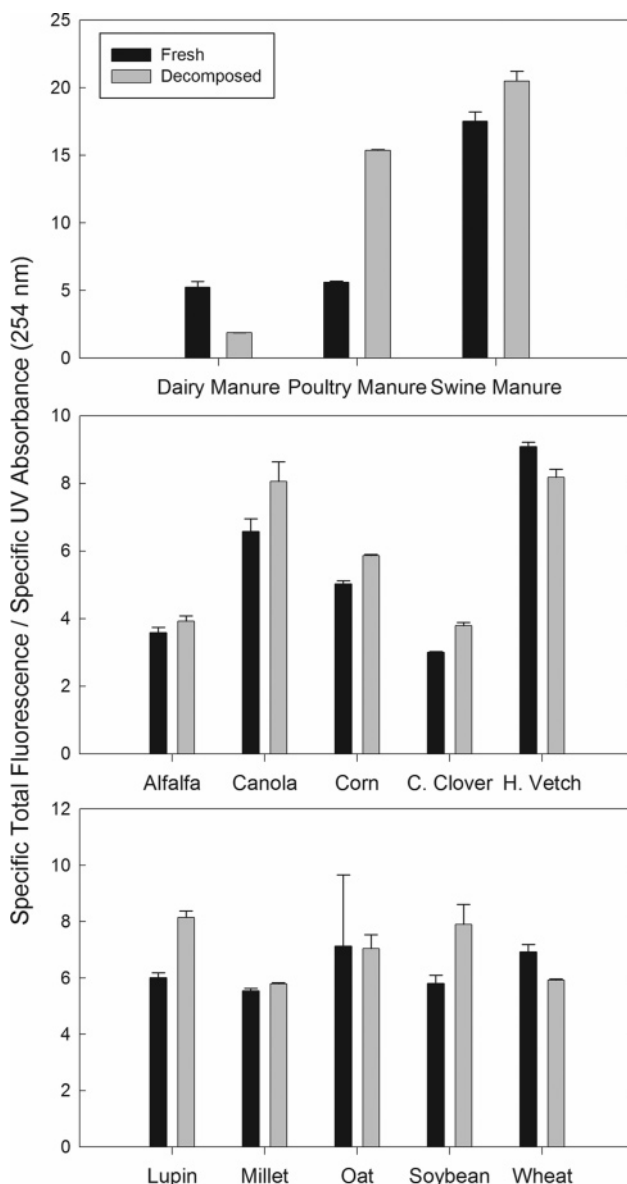
sample ID		DOC (mg L ⁻¹)	molar absorptivity at 280 nm	MW _{AP}	HIX
Non-Field-Weathered Plant Residues					
alfalfa	fresh	2360	94.9	632	1.98
	decomposed	2050*	113*	2610*	1.89 ^{NS}
canola	fresh	1140	69.0	270	1.03
	decomposed	820*	108*	648*	2.06*
crimson clover	fresh	3390	78.1	237	0.84
	decomposed	2330*	103*	353*	0.78*
hairy vetch	fresh	2370	50.2	277	0.97
	decomposed	1900*	118*	954*	1.30*
lupin	fresh	2130	45.2	240	0.93
	decomposed	1150*	86.2*	408*	1.51*
Field-Weathered Plant Residues					
corn	fresh	1710	88.0	595	1.55
	decomposed	1030*	163*	1640*	2.24*
millet	fresh	612	107	2170	1.25
	decomposed	370*	198*	6790*	2.43*
oat	fresh	721	117	1110	1.13
	decomposed	1260*	63.7*	2760*	1.01*
soybean	fresh	1160	65.7	690	1.36
	decomposed	882*	60.0 ^{NS}	2700*	1.46*
wheat	fresh	1510	72.9	1490	1.89
	decomposed	1040*	92.0*	2890*	2.33*
Animal Manure Residues					
dairy manure	fresh	424	376	6310	4.31
	decomposed	726*	411*	7240*	5.52*
poultry manure	fresh	957	293	242	2.06
	decomposed	987*	90.7*	5500*	3.21*
swine manure	fresh	1200	62.2	330	0.98
	decomposed	662*	111*	3250*	1.74*

^a * designates a significant difference at $p = 0.05$ between fresh and decomposed component concentrations for each extract. NS denotes nonsignificance.

components of higher aromaticity and/or MW_{AP} relative to that released from fresh residue material.

In studies that decompose DOM directly, increases in molar absorptivity with lower UV absorbance, possible when the C_{TS} content decreases concurrently, have generally been ascribed to the selective degradation of nonaromatic DOM components (17). Differentiating between selective degradation of less-complex DOM molecules and the release of more humified compounds into solution is not possible in the current study where the DOM was extracted from the residue following decomposition. Nevertheless, of the three DOM types that increased in C_{TS} content following residue decomposition, only that derived from dairy manure produced greater values of molar absorptivity, MW_{AP}, and HIX (Table 2). Thus, for dairy manure DOM, the increases in parameters related to humification could not have been caused by the degradation of DOM possessing lower MW_{AP} or lower absorptivity coefficients but rather must be due to the synthesis or release of higher MW_{AP}, more aromatic moieties into solution. Extracellular polymeric substances produced by microbial excretion and cell lysis are known to contain large (MW_{AP} >10000 Da), complex, and highly aromatic substances (11). The production of these materials during decomposition may be at least partly responsible for the very large increases in MW_{AP} and molar absorptivity observed following decomposition with some DOM samples, particularly those derived from animal manure residues.

Poultry manure-derived DOM has been previously observed to increase in C_{TS} content and decrease in molar absorptivity following decomposition. The increase in C_{TS} content was attributed to recalcitrant manure material becoming more soluble during the decomposition process, while the decrease in molar absorptivity observed was proposed as being due to the

**Figure 5.** Ratio of C_{TS}-normalized F/UV₂₅₄ at 254 nm for each of the DOM samples before and after decomposition.

degradation and loss, through ammonification, of polypeptides and/or nucleic acids from the fresh DOM (34). This study also shows a significant decrease in the molar absorptivity of poultry manure-derived DOM following decomposition. However, Table 1 shows that while the fluorescing components associated with the amino acids tryptophan and tyrosine (1 and 7) do decrease relative to the total fluorescence intensity following decomposition, they do not decrease in absolute concentration. Thus, the decrease in absorptivity observed with poultry manure-derived DOM following decomposition is most likely due to the loss of nucleic acids and not chromophoric amino acids and polypeptides.

Figure 5 illustrates the ratio of C_{TS}-normalized total fluorescence intensity to molar absorptivity (F/UV₂₅₄) for each of the DOM samples before and after decomposition. Because fluorophores generally represent some percentage of the overall solution aromaticity, the ratio of C_{TS}-normalized fluorescence to molar absorptivity provides a relative measure of the quantum efficiency (ratio of photons absorbed by a molecule to those emitted through fluorescence). For nine out of the 13 DOM solutions, the F/UV₂₅₄ ratio increases following decomposition, suggesting that fluorescing compounds are generally more

Table 3. Spearman Rank Correlation Coefficients between PARAFAC Components and Selected Chemical Characteristics with $n = 52^a$

PARAFAC component	dissolved organic carbon concn (DOC)	E2/E3 ratio	absorptivity at 280 nm	MW _{AP}	HIX
1	0.0316 ^{NS}	0.745 ^{***}	-0.0512 ^{NS}	-0.368 ^{**}	-0.392 ^{**}
2	-0.663 ^{***}	0.185 ^{NS}	0.679 ^{***}	0.580 ^{***}	0.786 ^{***}
3	-0.294 [*]	0.0686 ^{NS}	0.377 ^{***}	0.346 ^{**}	0.493 ^{***}
4	-0.620 ^{***}	0.311 [*]	0.577 ^{***}	0.443 ^{**}	0.652 ^{***}
5	-0.858 ^{***}	0.0867 ^{NS}	0.284 [*]	0.528 ^{***}	0.399 ^{**}
6	-0.428 ^{**}	-0.414 ^{**}	0.372 ^{**}	0.372 ^{**}	0.288 [*]
7	0.238 ^{NS}	0.382 ^{**}	0.0503 ^{NS}	0.157 ^{NS}	-0.0294 ^{NS}

^a *, **, and *** designate significant differences at $p = 0.05, 0.01, \text{ and } 0.001$. NS indicates that the correlation is not significant.

resistant to biodegradation than nonfluorescing UV-absorbing compounds. In their study of the biodegradation of effluent DOM, Saadi et al. (20) found analogous long-term increases in DOM F/UV₂₅₄ ratios after an initial period when F/UV₂₅₄ decreases. Similarly, Zanardi-Lamardo et al. (22) observed that DOM sampled from two Florida rivers contained fluorophores that were more resistant to degradation/removal processes than the nonfluorescing UV-absorbing components present.

These spectroscopic results suggest that the relationship between UV absorbance and fluorescence properties is complex and that the simultaneous use of both spectroscopic methods can provide complementary information. It is important to note that variations in DOM fluorescence component intensities may be due to many factors in addition to the formation or degradation of fluorophores. Although fluorescence intensity and emission wavelength maxima are intrinsic fluorophore properties, both are easily modified by changes to the molecular environment. Because of the complex heterogeneity of DOM components, changes to the molecular environment are difficult to predict since the nonfluorescing components of DOM (aliphatic organic acids, carbohydrates, and nonaromatic amino acids) may interact with fluorophores to an unknown extent. Metal complexation, molecular rigidity, and solution polarity all affect fluorophore molecular relaxation processes, which can result in altered fluorescence intensities and emission peak locations (35). For example, fluorophores contained within rigid macrostructures would be expected to have higher energy emissions than those same fluorophores held within flexible molecular structures. The decomposition process likely increases the complexity of the system under study by producing additional components capable of affecting DOM fluorescence. In general, carboxylic and phenolic functional group content, aromaticity, and molecular weight of DOM increased with decomposition of the DOM. These decomposition related changes, which presumably involve both fluorescing and nonfluorescing DOM fractions, likely affect molecular rigidity, complexation potential, and DOM polarity. In addition, denaturation of the tertiary structure of proteins during decomposition can lead to changes in the fluorescence characteristics of the aromatic amino acids tryptophan, tyrosine, and phenylalanine (35). Thus, as with all bulk chemical characterization methods, EEM spectroscopic analysis of DOM solutions has inherent limitations due to the complex interactions of the highly heterogeneous components present in a typical sample. By modeling the EEM data set into a limited number of spectral components, PARAFAC analysis likely reduces the noise associated with most minor molecular-level interactions.

Table 3 illustrates the Spearman rank-order correlation coefficients between selected chemical parameters and the PARAFAC fluorescent component scores. Tryptophan- and tyrosine-like components (1 and 7) showed either negative or no correlation with MW_{AP}, molar absorptivity, or HIX, which

is consistent with labile, low molecular weight (LMW) amino acids and polypeptides. These components did show rather strong correlation with the E2/E3 ratio, suggesting a relationship between these fluorophores and the lower MW_{AP} compounds. Regardless of their UV absorptivity, LMW organic and amino acids are poorly characterized by size exclusion methods. A UV absorbance proxy, such as the E2/E3 ratio, which relates absorbance at wavelengths associated with simple chromophores to absorbance associated with more complex chromophores, likely provides more information about these LMW DOM components. Component 2, although somewhat red-shifted, corresponds most closely in the literature to the humic acidlike components observed by Stedmon and Markager (31) as their component 3 and by Holbrook et al. (27) as their component 1. Component 4, on the other hand, corresponded closely with humic component "C" of Sheng and Yu (11). It is therefore consistent with the structural nature of humic acids that these components correlated most strongly with MW_{AP}, molar absorptivity, and HIX. The remaining three humic-like components also showed varying degrees of positive correlation with these parameters of humification. In addition, all humic-like components were negatively correlated with C_{TS} content, while components 1 and 7 were not significantly correlated with this parameter. This further indicates the importance of the role of decomposition in the formation of the humic-like fluorophores, since the C_{TS} concentration of most samples decreased significantly during this process. Correlation analysis shows that decomposition of the agricultural residues generally produced DOM of greater MW_{AP}, molar absorptivity, HIX, and humic-like fluorescence components. Previous studies have found strong correlation between these DOM parameters and the sorption to common soil minerals (2, 34). Excitation-emission fluorescence spectroscopy with PARAFAC may therefore provide an efficient, one-test method for predicting the sorptive capacity of agricultural residue extracts.

EEM fluorescence spectroscopy with PARAFAC is a sensitive, rapid, and nondestructive method of analysis capable of providing important structural information on DOM derived from agricultural residues. Seven individual fluorescence components were identified in the EEM spectra for a data set comprised of fresh and decomposed plant biomass and animal manure-derived DOM. Two out of seven of these peaks corresponded to known protein-like fluorophores, while four corresponded to known humic substance-like fluorescent components. Correlation was observed between these peaks and other spectroscopic characteristics such as MW_{AP}, molar absorptivity, and HIX. This study demonstrates that multidimensional fluorescence spectroscopy combined with PARAFAC can quantitatively characterize how microbial decomposition alters the chemical nature of DOM released from carbon-rich soil amendments such as crop residues, green manures, and animal manures.

ABBREVIATIONS USED

DOM, dissolved organic matter; MW_{AP}, apparent molecular weight; EEM, excitation–emission matrix; PARAFAC, parallel factor analysis; DI–H₂O, deionized distilled water; C_{TS}, total-soluble organic carbon; HIX, humification index; F/UV₂₅₄, total fluorescence intensity to molar absorptivity; LMW, low molecular weight.

LITERATURE CITED

- (1) Griffin, T. S.; Porter, G. A. Altering soil carbon and nitrogen stocks in intensively tilled two-year rotations. *Biol. Fertil. Soils* **2004**, *39*, 366–374.
- (2) Ohno, T.; Chorover, J.; Omoike, A.; Hunt, J. Molecular weight and humification index as a predictor of plant- and animal manure-derived dissolved organic matter to goethite. *Eur. J. Soil Sci.* **2006**, in press.
- (3) Aoyama, M. Use of high performance size exclusion chromatography to monitor the dynamics of water-soluble organic substances during the decomposition of plant residues in soil. *Soil Sci. Plant Nutr.* **1996**, *42*, 21–30.
- (4) Hur, J.; Schlautman, M. Molecular weight fractionation of humic substances by adsorption onto minerals. *J. Colloid Interface Sci.* **2003**, *264*, 313–321.
- (5) Chin, Y. P.; Aiken, G.; O’Laughlin, E. Molecular weight, polydispersity and spectroscopic properties of aquatic humic substances. *Environ. Sci. Technol.* **1994**, *28*, 1853–1858.
- (6) Guo, M.; Chorover, J. Transport and fractionation of dissolved organic matter in soil columns. *Soil Sci.* **2003**, *168*, 108–118.
- (7) Cox, L.; Celis, R.; Hermosin, M. C.; Cornejo, J.; Zsolnay, A.; Zeller, K. Effect of organic amendments on herbicide sorption as related to the nature of the dissolved organic matter. *Environ. Sci. Technol.* **2000**, *34*, 4600–4605.
- (8) Ohno, T. Fluorescence inner-filtering correction for determining the humification index of dissolved organic matter. *Environ. Sci. Technol.* **2002**, *36*, 742–746.
- (9) Boyd, T. J.; Osburn, C. L. Changes in CDOM fluorescence from allochthonous and autochthonous sources during tidal mixing and bacterial degradation in two coastal estuaries. *Mar. Chem.* **2004**, *89*, 189–210.
- (10) Baker, A.; Ward, D.; Lieten, S. H.; Periera, R.; Simpson, E. C.; Slater, M. Measurement of protein-like fluorescence in river and wastewater using a handheld spectrophotometer. *Water Res.* **2004**, *38*, 2934–2938.
- (11) Sheng, G. P.; Yu, H. Q. Characterization of extracellular polymeric substances of aerobic and anaerobic sludge using three-dimensional excitation and emission matrix fluorescence spectroscopy. *Water Res.* **2006**, *40*, 1233–1239.
- (12) Ohno, T.; Bro, R. Dissolved organic matter characterization using multiway spectral decomposition of fluorescence landscapes. *Soil Sci. Soc. Am. J.* **2006**, *70*, 2028–2037.
- (13) Merritt, K. A.; Erich, M. S. Influence of organic matter decomposition on soluble carbon and its copper binding capacity. *J. Environ. Qual.* **2003**, *32*, 2122–2131.
- (14) Corvasce, M.; Zsolnay, A.; D’Orazio, V.; Lopez, R.; Miano, T. M. Characterization of water extractable organic matter in a deep soil profile. *Chemosphere* **2006**, *62*, 1583–1590.
- (15) Sierra, M. M. D.; Giovanela, M.; Parlante, E.; Soriano-Sierra, E. J. Fluorescence fingerprint of fulvic and humic acids from varied origins as viewed by single-scan and excitation/emission matrix techniques. *Chemosphere* **2005**, *58*, 715–733.
- (16) Bertoncini, E. I.; D’Orazio, V.; Senesi, N.; Mattiazzo, M. E. Fluorescence analysis of humic and fulvic acids from two Brazilian oxisols as affected by biosolid amendment. *Anal. Bioanal. Chem.* **2005**, *381*, 1281–1288.
- (17) Kalbitz, K.; Schmerwitz, J.; Schwesig, D.; Matzner, E. Biodegradation of soil-derived dissolved organic matter as related to its properties. *Geoderma* **2003**, *113*, 273–291.
- (18) Marschner, B.; Kalbitz, K. Controls of bioavailability and biodegradability of dissolved organic matter in soils. *Geoderma* **2003**, *113*, 211–235.
- (19) Marschner, B.; Bredow, R. Temperature effects on release and ecologically relevant properties of dissolved organic carbon in sterilized and biologically active soils. *Soil Biol. Biochem.* **2002**, *33*, 805–813.
- (20) Saadi, I.; Borisover, M.; Armon, R.; Laor, Y. Monitoring of effluent DOM biodegradation using fluorescence, UV and DOC measurements. *Chemosphere* **2005**, *63*, 530–539.
- (21) Wu, F. C.; Tanoue, E.; Liu, C. Q. Fluorescence and amino acid characteristics of molecular size fractions of DOM in the waters of Lake Biwa. *Biogeochemistry* **2003**, *65*, 245–257.
- (22) Zanardi-Lamardo, E.; Moore, C. A.; Zika, R. G. Seasonal variation in molecular mass and optical properties of chromophoric dissolved organic material in coastal waters of southwest Florida. *Mar. Chem.* **2004**, *89*, 37–54.
- (23) Griffin, T. S.; Honeycutt, C. W. Using growing degree days to predict nitrogen availability from livestock manures. *Soil Sci. Soc. Am. J.* **2000**, *64*, 1876–1882.
- (24) Christensen, J. H.; Hansen, A. B.; Mortensen, J.; Andersen, O. Characterization and matching of oil samples using fluorescence spectroscopy and parallel factor analysis. *Anal. Chem.* **2005**, *77*, 2210–2217.
- (25) Bro, R.; Kiers, H. A. L. A new efficient method for determining the number of components in PARAFAC models. *J. Chemom.* **2003**, *17*, 274–286.
- (26) Judd, K. L.; Crump, B. C.; Kling, G. W. Variation in dissolved organic matter controls bacterial production and community composition. *Ecology* **2006**, *87*, 2068–2079.
- (27) Holbrook, R. D.; Yen, J. H.; Grizzard, T. J. Characterizing natural organic material from the Occoquan Watershed (Northern Virginia, US) using fluorescence spectroscopy and PARAFAC. *Sci. Total Environ.* **2000**, *361*, 249–266.
- (28) Cory, R. M.; McKnight, D. M. Fluorescence spectroscopy reveals ubiquitous presence of oxidized and reduced quinones in dissolved organic matter. *Environ. Sci. Technol.* **2005**, *39*, 8142–8149.
- (29) Alberts, J. J.; Takács, M. Total luminescence spectra of IHSS standard and reference fulvic acids, humic acids and natural organic matter: Comparison of aquatic and terrestrial source terms. *Org. Geochem.* **2004**, *35*, 243–256.
- (30) Leenheer, J. A.; Croué, J.-P. Characterizing dissolved aquatic organic matter. *Environ. Sci. Technol.* **2003**, *37*, 19A–26A.
- (31) Stedmon, C. A.; Markager, S. Resolving the variability in dissolved organic matter fluorescence in a temperate estuary and its catchment using PARAFAC analysis. *Limnol. Oceanogr.* **2005**, *50*, 686–697.
- (32) Yamashita, Y.; Tanoue, E. Chemical characterization of protein-like fluorophores in DOM in relation to aromatic amino acids. *Mar. Chem.* **2003**, *82*, 255–271.
- (33) Merchen, N. R. Digestion, absorption and excretion in ruminants. In *The Ruminant Animal: Digestive Physiology and Nutrition*; Church, D. C., Ed.; Waveland Press: Prospect Heights, IL, 1988; pp 172–201.
- (34) Hunt, J. F.; Ohno, O.; Zhongqi, H.; Honeycutt, C. W.; Dail, D. B. Influence of decomposition on chemical properties of plant- and manure derived dissolved organic matter and sorption to goethite. *J. Environ. Qual.* **2006**, in press.
- (35) Albani, J. R. *Structure and Dynamics of Macromolecules: Absorption and Fluorescence Studies*; Elsevier: New York, 2004; 414 pp.

Received for review November 17, 2006. Revised manuscript received January 5, 2007. Accepted January 8, 2007. This project was supported by National Research Initiative Competitive Grant 2003-35107-13628 from the U.S. Department of Agriculture Cooperative State Research, Education, and Extension Service and has also been supported by Hatch funds provided by the Maine Agricultural and Forest Experiment Station. This is MAFES Journal Paper #2928.